Biophysical Chemistry 153 (2010) 9–16

Contents lists available at ScienceDirect

Biophysical Chemistry

journal homepage: http://www.elsevier.com/locate/biophyschem

Defining the secondary structural requirements of a cocaine-binding aptamer by a thermodynamic and mutation study

Miguel A.D. Neves [1], Oren Reinstein, Makbul Saad, Philip E. Johnson *

Department of Chemistry, York University, 4700 Keele St., Toronto, Ontario, Canada M3J 1P3

ARTICLE INFO

Article history:
Received 30 July 2010
Received in revised form 9 September 2010
Accepted 9 September 2010
Available online 4 October 2010

ABSTRACT

Isothermal titration calorimetry (ITC) was used to measure the binding affinity and thermodynamics of a cocaine-binding aptamer as a function of pH and NaCl concentration. Tightest binding was achieved at a pH value of 7.4 and under conditions of no added NaCl. These data indicate that ionic interactions occur in the ligand binding mechanism. ITC was also used to measure the binding thermodynamics of a variety of sequence variants of the cocaine-binding aptamer that analyzed which regions and nucleotides of the aptamer are important for maintaining high-affinity binding. Individually, each of the three stems can be shortened, resulting in a reduced binding affinity. If all three stems are shortened, no binding occurs. If all three of the stems in the aptamer are lengthened by five base pairs ligand affinity increases. Changes in nucleotide identity at the three-way junction all decrease the affinity of the aptamer to cocaine. The greatest decrease in affinity results from changes that disrupt the GA base pairs and the identity of T19.

1. Introduction

The ability of aptamers to bind specifically and with high affinity to a variety of targets has spearheaded their development since their discovery in the early 1990s [1–4]. Aptamers have been selected to bind a wide range of ligands that vary from small molecules, to proteins to whole cells. Aptamers are typically developed to act as biosensors, but have also gained therapeutic use [4]. Despite the interest shown in aptamers for medicinal and biotechnology uses, relatively few studies have focused on the biochemistry and biophysics of how aptamers function.

The cocaine-binding aptamer has become a well-developed template for a wide range of different biosensor technology. This aptamer is composed of three stem loops that meet at three-way junction (Fig. 1a) [5]. In contrast to the reported secondary structures of most other aptamers, the cocaine-binding aptamer has few single-stranded regions. The different sensing technologies to exploit the cocaine-binding aptamer function include optical, electrochemical as well as spectroscopic reporting of ligand binding [6–17]. One reason there is such a widespread utilization of the cocaine-binding aptamer scaffold is that this molecule can be engineered to follow a structural switching or ligand-induced folding mechanism. When stem 1 is shortened to contain three base pairs the resulting aptamer is unfolded when free and ligand binding induces folding [18,19]. A second method to achieve ligand-induced folding is to divide the aptamer into two separate strands. Cocaine binding results in the assembly of the two strands and the ligand into a single tertiary complex [5]. This ability has been recently exploited to control the assembly of a variety of DNA-based supramolecular complexes [20–22]. In this study we use isothermal titration calorimetry (ITC) to gain insight into the ligand binding mechanism of the cocaine-binding aptamer by studying ligand binding as a function of both pH and NaCl conditions. We also use ITC to study the binding of a series of cocaine-binding aptamer variants in order gauge which regions and nucleotides are important for ligand binding.

2. Materials and methods

Aptamer samples were obtained from the University of Calgary DNA Service. DNA samples for ITC experiments were exchanged with 20 mM Tris (pH 7.4), 140 mM NaCl, 5 mM KCl, or other buffer condition, three times before use. Cocaine hydrochloride was obtained from Sigma-Aldrich.

All 1D-^{1}H NMR experiments on aptamer samples were acquired using a 600 MHz Bruker Avance spectrometer. 1D-^{1}H NMR spectra were acquired in 90% H_2O/10% ^2H_2O at 5 °C unless otherwise noted. Cocaine concentrations were determined by weight. Aptamer concentrations were determined by absorbance spectroscopy using the calculated extinction coefficients. The concentrations of aptamers for NMR studies ranged from 0.5–2.3 mM. Data were processed and analyzed using NMRPipe/NMRDraw [23].

Abbreviations: ΔC_p, change in heat capacity; K_d, dissociation constant; NMR, nuclear magnetic resonance; ITC, isothermal titration calorimetry.

* Corresponding author. Tel.: +1 416 736 2100x3319; fax: +1 416 736 5936.
E-mail address: pjohnson@yorku.ca (P.E. Johnson).
[1] Current address: Department of Chemistry, University of Toronto, Toronto, Ontario, Canada.

0301-4622/$ – see front matter © 2010 Elsevier B.V. All rights reserved.
doi:10.1016/j.bpc.2010.09.009

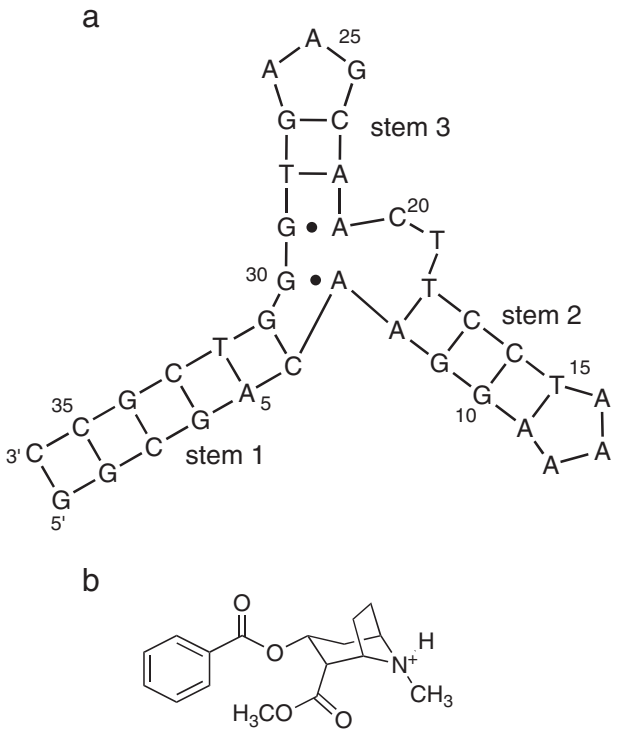

Fig. 1. (a) sequence and secondary structure of the MN4 cocaine-binding aptamer. Dashes between nucleotides indicate Watson–Crick base pairs. Dots indicate non-Watson–Crick base pairs. (b) chemical structure of cocaine. Shown is the protonated and positively charged form as is expected to exist at pH 7.4.

Isothermal titration calorimetry (ITC) was performed using a MicroCal VP-ITC. The data was analyzed using the packaged Origin software and fit to a one-site binding model. Samples for ITC analysis were degassed before use with the MicroCal Thermo Vac unit. All experiments were corrected for the heat of dilution of the titrant. Unless otherwise specified, cocaine and aptamer solutions were prepared in a buffer of 20 mM Tris (pH 7.4), 140 mM NaCl, 5 mM KCl. Binding experiments were typically performed with aptamer solutions of 20 μM using cocaine concentrations of 280 μM at 20 °C. For binding studies conducted at pH 5.4 and 6.4, buffers of 20 mM sodium acetate and sodium phosphate, respectively, were used and contained the same NaCl and KCl conditions as stated above. Binding studies above pH 7.4 were conducted in 20 mM Tris at the indicated pH. Experiments conducted where the NaCl concentration was varied were conducted with the aptamer in pH 7.4 Tris buffer containing the indicated amount of NaCl. All aptamer samples were heated in a boiling water bath for three minutes and cooled in ice-water prior to use in an ITC experiment to allow the aptamer to anneal. Binding experiments typically consisted of either (i) 30 successive 8 μL injections of cocaine every 300 s to a final molar ratio of 2.5:1. Or (ii) 36 injections of 6 μL cocaine spaced every 300 s to a final molar ratio of 2:1. For all experiments, the first injection volume was 1 μL. The raw ITC data was corrected for heat of dilution of the titrant.

Some constructs only bind weakly at these aptamer and cocaine concentrations due to low affinity of the aptamer for ligand. A low c ITC method was developed for these constructs [24,25]. For low c ITC experiments the running conditions were kept the same, however these experiments consisted of 35 successive injections of 45 mM cocaine. The first 10 injections were 5 μL and the remaining additions were 8 μL injected every 300 s to a 50 fold molar excess of cocaine. The raw low c data was also corrected for heat of dilution of the titrant. The constructs fit under these low c conditions are WC, MN5, MN6, MN7, MN9, MN10, MN11, MN13, M14 and MN17. For constructs MN15 and MN16 even lower c conditions were attempted using a 400:1 molar ligand excess.

For the two-stranded aptamer, two experiments were carried out. First, MS3 was titrated into MS4 where the concentrations were 213 μM and 20 μM, respectively. ITC experiments consisted of 35 successive injections spaced every 360 s where the first injection was 1 μL, the next 20 injections were 3 μL, and the last 14 injections were 15 μL. The final molar ratio was a 2.25 fold excess of cocaine. For the titration of cocaine into a 1:1 molar ratio of MS3 and MS4 the concentration of each DNA strand was 40 μM and the concentration of cocaine used was 0.57 mM. ITC experiments consisted of 35 successive injections spaced every 360 s where the first injection was 1 μL, the next 20 injections were 3 μL, and the last 14 injections were 15 μL. The final molar ratio was a 2.75 fold excess of cocaine. ITC experiments involving MS3 and MS4 were performed at 15 °C.

3. Results

3.1. Effect of pH on cocaine binding

In order to determine the optimal pH value for cocaine binding and investigate the role played by titrateable groups on either the ligand or aptamer, the binding ability of the MN1 aptamer was determined as a function of pH value. Binding was studied at pH values of 5.4, 6.4, 7.4, 9.2 and 9.6 (Table 1). Tightest binding was observed at pH 7.4. At pH values both higher and lower than 7.4 we observe weaker binding. At pH 9.6 we observed no appreciable binding and we give an estimate that binding must be weaker than approximately 2 mM.

3.2. Effect of ionic strength on cocaine binding

At a pH value of 7.4, the optimal value for binding, the amine in cocaine is expected to be protonated (Fig. 1b) [26]. The importance of the positive charge in aptamer-binding can be assayed by measuring binding as a function of ionic strength. The cocaine-binding parameters of MN1 and MN4 at NaCl concentrations from 0 to 1 M are shown in Table 2 and representative ITC data is shown in Fig. 2. Both MN1 and MN4 show a similar trend of having maximum binding affinity when no NaCl is present. A maximum binding affinity of (0.3 ± 0.1) μM is observed for MN4 with the condition of 0 mM NaCl. For MN1 with no added NaCl, the affinity is (1.4 ± 0.3) μM. At higher NaCl concentrations binding weakens. Binding affinity decreases to 31 ± 1 μM for MN1 in the presence of 500 mM NaCl. Further increases in NaCl concentration to 1 M did not significantly weaken the binding affinity of MN1. At each NaCl concentration studied, binding is enthalpically driven and compensated with an unfavorable binding entropy (Table 2).

To test if the differences in cocaine binding affinity we observe for the aptamer in the presence and absence of NaCl were due to salt-induced structural changes, we monitored the imino proton 1D NMR spectrum of MN4 as NaCl was added (Fig. 3). As the concentration of NaCl increases, the linewidths of the imino protons increase, but the resonances stay at the same chemical shift. This indicates no structural

Table 1
pH dependence of the dissociation constant and thermodynamic parameters of cocaine binding for the aptamers MN1[a].

pH	n	K_d (μM)	ΔH (kcal mol^{-1})	−TΔS (kcal mol^{-1})
5.4	0.80	13.0 ± 0.7	-18.2 ± 0.5	11.7 ± 0.5
6.4	0.86	13.9 ± 0.1	-23 ± 1	16 ± 1
7.4	0.88	9.15 ± 0.09	-28.1 ± 0.7	21.1 ± 0.7
9.2	0.65	22.9 ± 0.9	-11.0 ± 0.8	4.8 ± 0.8
9.6	nd	>2 mM	nd	nd

[a] Data acquired at 20 °C at the indicated pH with 140 mM NaCl, 5 mM KCl. The values reported are averages of 2–4 individual experiments. The error range reported is one standard deviation. nd indicates that the value was not determined.

Table 2
Ionic strength dependence of the dissociation constant and thermodynamic parameters of cocaine binding for aptamers MN1 and MN4[a].

[NaCl] (mM)	n	MN1		−TΔS (kcal mol^{-1})	[NaCl] (mM)	n	MN4		−TΔS (kcal mol^{-1})
		K_d (μM)	ΔH (kcal mol^{-1})				K_d (μM)	ΔH (kcal mol^{-1})	
0	0.80	1.4 ± 0.3	−22.7 ± 1.7	14.8 ± 1.9	0	0.80	0.3 ± 0.1	−16 ± 3	9.3 ± 0.8
140	0.88	9.15 ± 0.09	−28.1 ± 0.7	21.1 ± 0.7	140	0.84	7 ± 1	−14.5 ± 0.4	7.6 ± 0.5
500	0.68	31 ± 1	−21.2 ± 0.7	15.2 ± 0.7	500	0.89	35 ± 8	−8.4 ± 0.8	2.4 ± 0.7
1000	0.60	27 ± 3	−12.5 ± 0.6	6.3 ± 0.5					

[a] Data acquired at 20 °C in 20 mM Tris (pH 7.4) with the amount of NaCl indicated. The values reported are averages of 2–4 individual experiments. The error range reported is one standard deviation.

changes occur as the salt concentration increases. Instead, the increase in linewidth reflects a change in dynamics of the aptamer with the addition of NaCl.

3.3. Binding analysis of aptamer variants

We analyzed the importance of the length of the three stems of the cocaine-binding aptamer by varying stem length and measuring the cocaine binding affinity of these constructs (Fig. 4). When stem 3 was eliminated or shortened by two base pairs (S1S2, SS3 and MN2), cocaine binding was eliminated. For the MN5 construct, where stem 3 is shortened by one base pair, missing only the GT base pair adjacent to the triloop, binding occurs but the affinity is reduced to 42 ± 4 μM (Table 3). Stem 2 can be shortened to contain a single putative base pair (MN7) and still retain cocaine binding with a reduced affinity of 55 ± 1 μM (Table 3). Previously, we and others showed that stem 1 can be shortened to consist of three base pairs and still retain reasonable affinity (MN6 and MN19) [18,19] (Fig. 4; Table 3). We also tried to combine the length decrease in all three stems to test the additivity effect of shortening all of the stems. The construct MN18 combined the stem shortening mutations of MN5, MN7 and MN6 and the resulting molecule displayed no detectable ligand binding.

The importance of the identity of the noncanonical base pairs for cocaine binding was also analyzed. When all the noncanonical base pairs in the cocaine-binding aptamer, as drawn with the original proposed secondary structure [5] are changed to Watson-Crick base pairs (construct WC; Fig. 4) binding is reduced 23 fold to 204 ± 6 μM. This large reduction in binding showed the importance of the noncanonical base pairs in cocaine binding. But are all the non-canonical base pairs important, or just some? To determine this we tested the mutants MN3, MN4 and MN8 (Fig. 4). These variants had affinities of 14 ± 4 μM, 7 ± 1 μM, and 8.6 ± 0.2 μM, respectively. All of these constructs bind with a very similar affinity as the original MN1 aptamer and show that the predicted T23/G27, G2/A35 and A3/G34 base pairs in MN1 are not essential for high affinity binding. In contrast, analysis of MN9, MN10, and MN11 show the importance of the noncanonical G29/A21 base pair. When this GA base pair is modified to be a GC base pair, binding was greatly reduced to values of 193 ± 1 μM, 148 ± 9 μM and 123 ± 22 μM for MN9, MN10 and MN11, respectively. The importance to binding of the G30/A7 base pair was assayed by construct MN12 (Fig. 4). In MN12, A7 was changed to a C resulting in a G30/C7 base pair in place of the G30/A7 base pair. For MN12 no binding was observed, even under the low c conditions used to assay weak binders. This indicates that the identity of A7, and retaining the A7/G30 base pair, is essential to maintain aptamer function.

In the secondary structure of the cocaine-binding aptamer there are two unpaired nucleotides present at the three-way junction, T19 and C20. The importance of the identity of these two residues for cocaine binding was tested in constructs MN15, MN16 and MN17

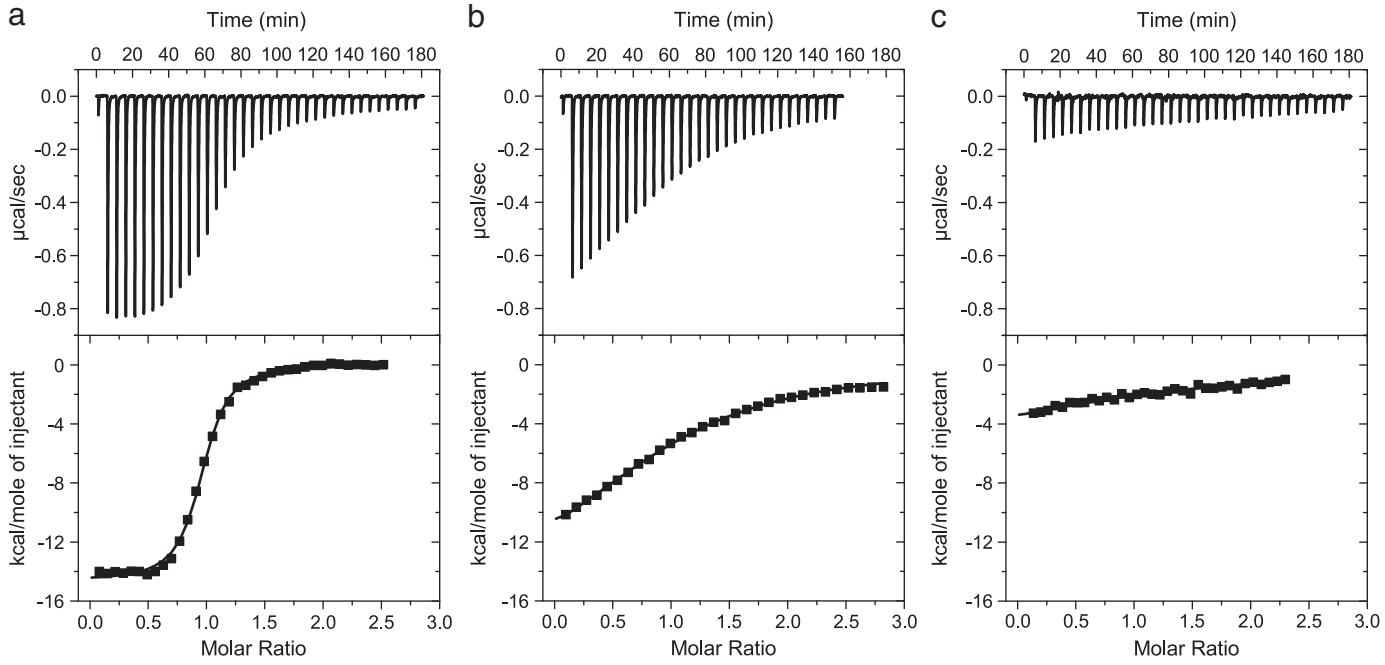

Fig. 2. Analysis of cocaine binding by the MN4 aptamer using isothermal titration calorimetry. Shown are titrations of cocaine into an MN4 aptamer solution in the presence of (a) 0 mM NaCl, 20 mM Tris, pH 7.4, (b) 140 mM NaCl, 20 mM Tris, pH 7.4 and (c) 500 mM NaCl, 20 mM Tris, pH 7.4. On top is the raw titration data showing the heat resulting from each injection of cocaine into the aptamer solution. On the bottom are the integrated heats after correcting for the heat of dilution. Binding affinity increased, with K_d values changing from 35 ± 8 μM to 7 ± 1 μM to 0.3 ± 0.1 μM as the concentration of NaCl decreased from 500 mM to 140 mM to 0 mM.

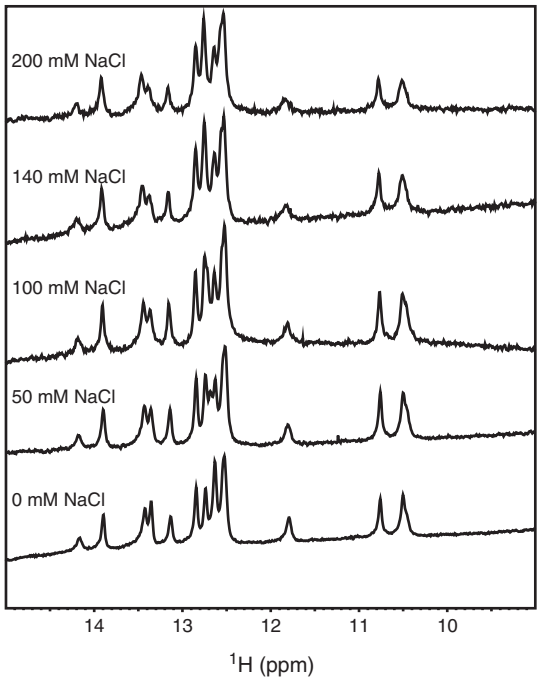

Fig. 3. Change in the imino proton NMR spectrum of the MN4 aptamer as a function of added NaCl. Shown are the 1D ^{1}H NMR spectra of cocaine-bound MN4 in conditions of 0 to 500 mM NaCl. The signal to noise decreases as NaCl is added but the resonances do not significantly change chemical shift indicating that addition of NaCl does not cause structural changes in the aptamer.

(Fig. 4). In MN17, C20 was replaced by a G. MN17 retained binding but with a reduced affinity of 59 ± 13 μM, 8.4 times lower than for MN4. In MN16, T19 is replaced by an A nucleotide. This change resulted in no quantifiable binding being observed for this construct. Changes in the thermogram with ligand binding under low c conditions indicated that very weak binding, in the millimolar range, was occurring. Similar very weak binding was observed for MN15 where a double mutant (T19 to C; C20 to T) was tested. Together these results indicate that the identity of T19 is critical to maintain cocaine binding while the identity of C20 is less critical.

From the NMR imino proton chemical shift perturbations measured upon cocaine binding we observed that G31 and T32 experienced the greatest change in chemical shift with ligand binding [18]. Compensatory mutations at these positions in the MN4 sequence were analyzed to test the importance of these nucleotides for ligand recognition. In MN13 the G31/C6 base pair was switched to be C31/G6. In this construct weak binding was maintained at 211 ± 25 μM, a level 30 fold weaker than for MN4. This indicates that the spatial positioning of the G and C nucleotides in the G31/C6 base pair is important to maintain high-affinity binding. For MN14 the T32/A5 base pair was reversed to be a A32/T5 base pair. In this construct, fairly tight binding was maintained at 31 ± 5 μM, yet this is still over 4 fold lower than observed for MN4.

From the chemical shift perturbation data, the imino proton of T18 showed little change with ligand binding indicating it may be away from the site of cocaine binding. This was tested in construct MN20 where both AT base pairs in stem 2 were changed to be GC base pairs. Additionally, this construct had a shortened stem 1 and the AT base pair adjacent to the triloop in stem 3 changed to be GC as in MN19. MN20 binds cocaine with a K_d of 13 ± 7 μM, roughly twice as tight as the MN19 aptamer it was based on. As MN20 has a short stem 1 we used NMR methods to see if it transforms from an unfolded to folded structure with ligand binding. The 1D-^{1}H NMR of the free MN20 shows 5–6 peaks. This indicates that this aptamer is not fully folded in the free state. In the bound form there are the expected 12 imino peaks from the folded aptamer with three stem loops showing that ligand-induced folding occurs with MN20 (Fig. 1 of the supplementary material). We also gauged the thermal stability of MN20 by recording ^{1}H 1D spectra as a function of temperature (Fig. 2 of the supplementary material). The last temperature at which a signal is visible in the bound MN20 aptamer is 30 °C.

Finally, the cocaine binding ability of an aptamer in which all three stems have been lengthened by five base pairs (MN21) was measured (Fig. 4). This aptamer has the tightest affinity for cocaine of any aptamer variant we have studied to date, having a K_d of 4 ± 1 μM, in the standard buffer conditions (Table 3).

3.4. Binding analysis of a two-stranded cocaine-binding aptamer

Many of the biotechnology applications of the cocaine-binding aptamer rely on a structural switching mechanism where the aptamer has been divided into two separate strands and cocaine binding assembles the complex (Fig. 5) [5]. We used ITC to analyze this binding mechanism in terms of the affinity of the two strands for each other, and of a 1:1 molar ratio mixture of the two strands for cocaine. The two DNA strands MS3 and MS4 bind each other with a K_d value of 11 ± 1 μM, a ΔH value of -48 ± 2 kcal mol^{-1} and a ΔS value of -142.4 cal mol^{-1} K^{-1}. A 1:1 molar ratio of MS3 to MS4 binds cocaine with an affinity of 6 ± 1 μM, a ΔH value of -12 ± 2 kcal mol^{-1} and a ΔS value of -20 ± 5 cal mol^{-1} K^{-1}.

4. Discussion

4.1. Effect of buffer conditions on cocaine binding

Both the ligand, cocaine, and the DNA aptamer contain titrateable groups (Fig. 1b). In order to see what effect protonation of these groups may have on cocaine binding, the MN1 aptamer was analyzed by measuring the binding thermodynamics as a function of pH. The optimal pH value for binding is 7.4. Below this value, binding affinity is slightly decreased. This decrease may result from the change in the buffer used. Above pH 7.4, binding is more significantly decreased. Cocaine is a secondary amine and has an experimentally determined pK_a value of 8.6 and a calculated pK_a value of 8.01 to 9.00 depending on the prediction method used [26]. The decreased binding affinity at pH 9.2 is consistent with deprotonation of the cocaine resulting in a lower affinity and suggests that cocaine needs to be positively charged in order to take advantage of ionic interactions to obtain maximum affinity. The lack of observable binding at pH 9.6 likely results from a combination of having a fully deprotonated cocaine ligand and also potential deprotonation of the guanine imino proton that has a pK_a value of 9.2. Changing the protonation of the guanines will almost certainly have a very disruptive effect on the structure of the cocaine-binding aptamer.

Having the cocaine protonated suggests that ionic interactions are involved in the cocaine binding mechanism. This interaction most likely involves the negative phosphate backbone of the DNA interacting with the positive charge on cocaine. We further tested the importance of ionic interactions by measuring binding affinity as a function of added NaCl. As seen in Table 2 binding affinity decreases as NaCl concentration increases for both aptamers studied. We observe a

Fig. 4. Sequence and secondary structures of the different cocaine-binding aptamer constructs analyzed. Nucleotides that are altered compared to MN1 are colored red. The binding affinity determined for each construct is indicated under the name. K_d values in bold indicate constructs with affinities much weaker (greater than 100 μM) than that of MN1. For legibility, the error in the K_d value is not included here but is given in Table 3. nbd denotes no binding detected. vwb indicates very weak binding detected, but was not quantifiable.

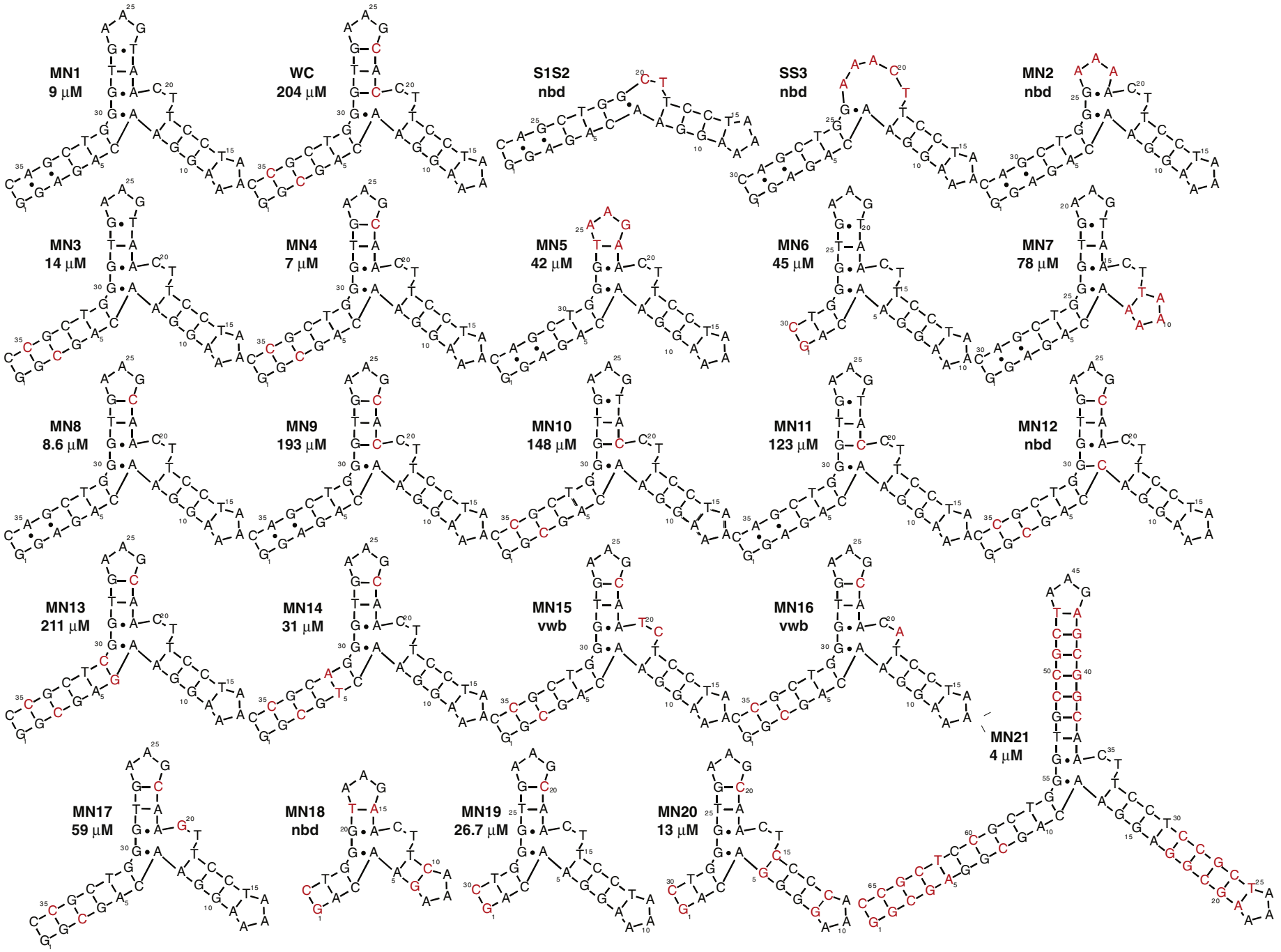
MN1
9 μM
WC
204 μM
S1S2
nbd
SS3
nbd
MN2
nbd
MN3
14 μM
MN4
7 μM
MN5
42 μM
MN6
45 μM
MN7
78 μM
MN8
8.6 μM
MN9
193 μM
MN10
148 μM
MN11
123 μM
MN12
nbd
MN13
211 μM
MN14
31 μM
MN15
vwb
MN16
vwb
MN21
4 μM
MN17
59 μM
MN18
nbd
MN19
26.7 μM
MN20
13 μM

Table 3
The binding affinity and thermodynamic binding parameters of ligand binding by cocaine aptamer constructs as determined by isothermal titration calorimetry.[a]

Aptamer	n	K_d (μM)	ΔH (kcal mol^{-1})	−TΔS (kcal mol^{-1})
MN1[b]	0.88	9.15 ± 0.09	−28.1 ± 0.7	21.1 ± 0.7
WC	1[e]	204 ± 6	−12.5 ± 0.9	7.6 ± 0.9
S1S2		nbd[c]		
SS3		nbd		
MN2		nbd		
MN3	1.09	14 ± 4	−13.84 ± 0.01	7.3 ± 0.2
MN4[b]	0.84	7 ± 1	−14.5 ± 0.4	7.6 ± 0.5
MN5	1[e]	42 ± 4	−8.5 ± 0.4	2.6 ± 0.4
MN6[b]	1[e]	45.3 ± 0.5	−22 ± 2	16 ± 2
MN7	1[e]	55 ± 1	−9.9 ± 0.2	4.2 ± 0.2
MN8	0.75	8.6 ± 0.2	−13.4 ± 0.5	6.6 ± 0.5
MN9	1[e]	193 ± 1	−5.23 ± 0.01	0.25 ± 0.02
MN10	1[e]	148 ± 9	−15.6 ± 0.9	10.5 ± 0.9
MN11	1[e]	123 ± 22	−12.8 ± 0.2	7.46 ± 0.01
MN12		nbd		
MN13	1[e]	211 ± 25	−6.7 ± 0.4	1.8 ± 0.4
MN14	1[e]	31 ± 5	−5.4 ± 0.3	0.6 ± 0.2
MN15		very weak binding[d]		
MN16		very weak binding		
MN17	1[e]	59 ± 13	−8.7 ± 0.2	3.0 ± 0.3
MN18		nbd		
MN19[b]	0.81	26.7 ± 0.7	−23.9 ± 0.9	17.7 ± 0.9
MN20	0.85	13 ± 7	−16 ± 2	10 ± 2
MN21	0.4	4 ± 1	−20.1 ± 1	12 ± 1

[a] Data acquired at 20 °C in 20 mM Tris (pH 7.4), 140 mM NaCl and 5 mM KCl. The values reported are averages of 2–4 individual experiments. The error range reported is one standard deviation.
[b] These data are from Neves et al. [18].
[c] nbd indicates no binding was detected even under low c ITC conditions.
[d] Binding detected but data could not be fit. Very weak binding, on the order of millimolar, is estimated.
[e] Data fit under low c conditions and n was restrained to be 1.

22 and 117 fold reduction in affinity between conditions of 0 and 500 mM NaCl, for MN1 and MN4 respectively. This reduced affinity indicates that charge-dependant interactions are important for achieving tight binding as added NaCl should shield ionic interactions and weaken binding. However, as binding still occurs at high NaCl concentrations cocaine binding by these aptamers is not entirely driven by ionic interactions. Taken together, the results of altering pH and NaCl conditions show that ionic interactions play a role in cocaine-DNA interactions, but that this is not the only type of intermolecular interactions governing ligand binding.

We will also note that tightest binding was achieved at pH 7.4, the pH at which the aptamer was originally selected [5]. Additionally, binding was tightest with no NaCl present. This is a little surprising as the aptamer was selected at a NaCl concentration of 140 mM and aptamer binding is often thought to be tightest under the same conditions as selection occurs. For other aptamers where ionic interactions are thought to occur, binding conditions of lower NaCl concentration than originally used for selection should be tested if an increased affinity for the target is desired.

4.2. Importance of stem length and nucleotide identity in cocaine binding

In order to see which regions of the aptamer and which nucleotides are important for aptamer function we analyzed the cocaine binding ability of a series of cocaine-binding aptamers (Table 3; Fig. 4). We first changed the length of each of the three stems in the cocaine-binding aptamer. We found that on an individual basis, each of the three stems can be shortened by one to three base pairs from their original length and still retain reasonable binding affinity. We define reasonable affinity as not more than ~10 fold weaker than observed for MN1. When combined into a single construct, MN18, the combination of the detrimental effects on binding reduced the affinity of MN18 for cocaine to a level lower than we could measure. These data show that in order to retain high-affinity binding the stem length needs to be maintained at the length of the originally selected aptamer.

We also tested a construct where the length of each of the stems is increased by five new base pairs (MN21). This change doubles the length of each of the stems. In a previous study we showed that MN4 undergoes very little or no change in secondary structure with ligand binding and that binding is accompanied by a more negative change in heat capacity of binding (ΔC_p) than predicted to occur based solely on ligand burial [18]. We suggested a binding mechanism in which tertiary structural changes occur for MN4, and the packing of the three helices provides a positive driving force for binding. We reasoned that by increasing the length of the stems, this would result in an increase in driving force and result in an increase in ligand affinity. Consistent with this hypothesis we did observe a 1.75 fold increase in affinity for MN21 compared to the shorter stem length MN4. We did not further test this with additional constructs with even longer stems, but we would expect a further modest increase in affinity as the length of the three stems increase.

Our binding results on individual nucleotide changes in the cocaine-binding aptamer variants presented here are consistent with previously published data on the binding ability of cocaine-binding aptamer mutants. When adapting the cocaine-binding aptamer for use in steroid binding, numerous sequence variants of the aptamer were assayed for cocaine binding [27–29]. In these studies, cocaine-binding aptamer variants where the G29/A21 base pair was changed to a GC base pair, no cocaine binding was reported [27]. In our results, a mutation disrupting the same base pair (WC, MN9, MN10, MN11) results in a greatly reduced binding affinity, 14 to 23 fold, compared to MN1. Additionally, for aptamers where double mutations were introduced that disrupted the G30-A7 base pair and altered the identity of T19, cocaine binding was eliminated [28]. Our binding studies with constructs MN12 and MN16 contained similar changes and the cocaine binding ability of these aptamers was similarly eliminated or greatly weakened.

The cocaine-binding aptamer core contains a tandem arrangement of GA base pairs. In a crystal structure of a tandem GA arrangement, the mismatch caused the B-form helix to kink toward the major groove side and extensive inter-strand base stacking was observed at the GA mismatch [30]. In the cocaine-binding aptamer the tandem GA mismatch likely imparts a conformation in the DNA structure required for ligand binding. This is evident in our mutational data. In constructs where the G29-A21 base pair was disrupted (WC, MN9, MN10, MN11) binding affinity was decreased 14 to 23 times compared to MN1. When the G30-A7 base pair was disrupted (MN12) no binding was observed. Mutations in the GA base pairs likely result in a structural change in the aptamer that prevents the aptamer binding cocaine. An alternate possibility is that the GA base pairs make direct contact with cocaine and that the A to C mutations introduced alter the atoms that interact with cocaine. An argument against this second possibility is that the imino protons of G29 and G30 experience only a relatively small change in chemical shift with cocaine binding [18]. The residues that change the most in chemical shift with cocaine binding are G31 and T32. The importance of the imino of T19 is shown by the observation that it is only observable in the ligand-bound form. It is possible that T19 directly contacts cocaine with the imino proton becoming protected from hydrogen exchange upon ligand binding. Consistent with this proposal, in the construct MN16 where T19 is changed to an A, cocaine binding by the aptamer is eliminated. It is possible that T19 is important for structural reasons in addition to, or instead of making contact with the cocaine ligand. The large chemical shift change with ligand binding seen in G31 likely comes from this base pair directly contacting the ligand, the compensatory mutant where the G31-C6 base pair is changed to C31-G6 (MN13) results in a 30 fold decrease in binding affinity when compared to MN4.

Binding of MN20 shows that changing the two AT base pairs in stem 2 to GC base pairs results in a moderate increase in affinity of the

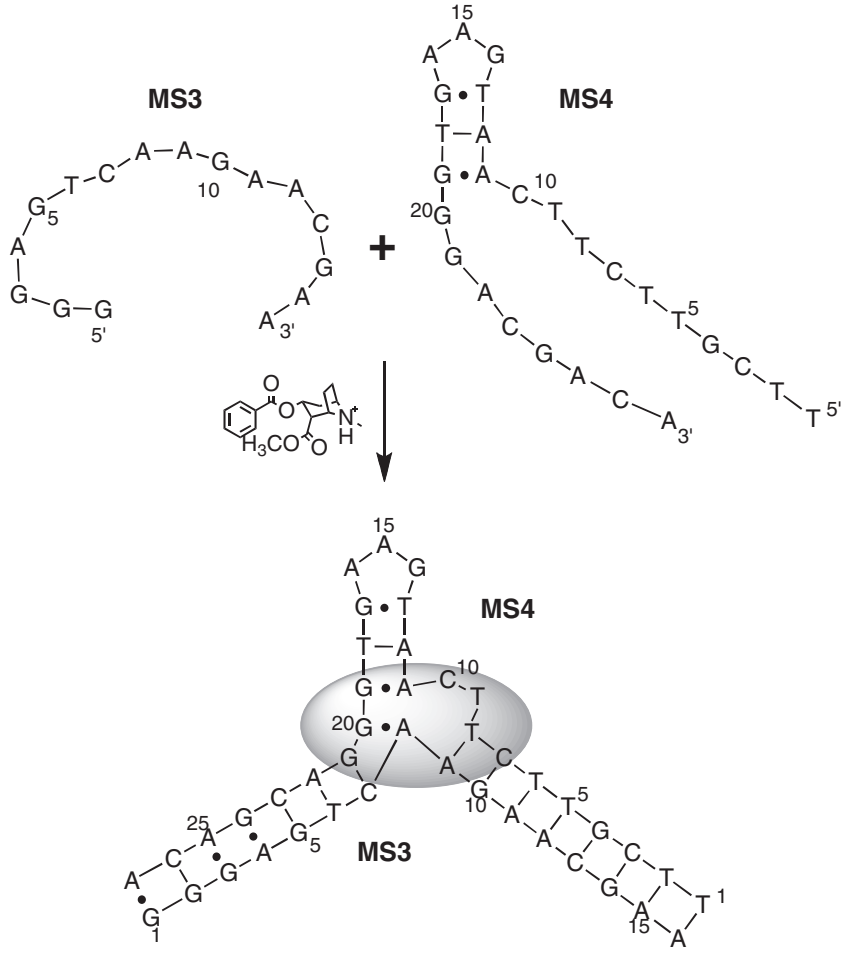

Fig. 5. Ligand-induced folding mechanism of a two-stranded cocaine-binding aptamer. The sequences of MS3 and MS4 are shown.

aptamer compared to MN19, on which it was based. As the imino proton chemical shift perturbation of residues in this stem are small [18] we did not expect these changes to hinder binding. We initially thought this increase in affinity resulted from an increase in stability of the free aptamer, but the temperature at which the last imino is visible in a 1D ^{1}H NMR spectrum is unchanged from MN19 to MN20 (Fig. 2 of the supplementary material). It is possible that the affinity increase is derived from an increase in the mount of secondary structure of the unbound state of MN20 compared to that of MN19. Consistent with this, there are more imino protons present in the free form of MN20 compared to MN19. Additionally, the enthalpy of binding is lower for MN20 compared to MN19 (Table 3) possibly due to fewer hydrogen bonds forming upon folding. This is offset by a lower unfavorable binding entropy possibly due to a higher degree of organization in the free state. While such arguments may be valid in this case, the analysis of binding thermodynamics are complicated by hydration effects and similar arguments may not be valid in other cases.

From a comparison of the enthalpy and entropy values with the affinity data (Table 3) for the different aptamers, insights into which of these thermodynamic parameters are important or not important for binding can be made. For the tightest binding constructs, $K_d < 100$ μM, the enthalpy and entropy values highly vary. The enthalpy values can range from -28.1 ± 0.7 kcal mol^{-1} for MN1 to -5.4 ± 0.3 kcal mol^{-1} for MN14 while the $-T\Delta S$ values range from 21.1 ± 0.7 kcal mol^{-1} to 0.6 ± 0.2 kcal mol^{-1} for MN1 and MN14, respectively. In contrast, for the constructs that bind cocaine the weakest, $K_d > 100$ μM, there is not as large of a variation in enthalpy and entropy values. For the weakly binding aptamers, the entropy values are not among the most exothermic observed for these aptamers and range from -15.6 ± 0.9 kcal mol^{-1} to -5.23 ± 0.01 kcal mol^{-1} for MN10 and MN9, respectively. The corresponding values of $-T\Delta S$ do not include the most unfavorable values and range from 10.5 ± 0.9 kcal mol^{-1} to 0.25 ± 0.02 kcal mol^{-1} for MN10 and MN9, respectively.

As shown in Table 3, binding data for many of the constructs were acquired with low c conditions. When fitting these data to determine the affinity and binding enthalpy we fixed the n value to be 1 [25]. While we include the enthalpy values here we will note that the optimal method to determine ΔH° recommended by Tellinghuisen involves repeating binding at a variety of temperatures and obtaining ΔH° from a van't Hoff analysis. Using this n value is valid for two reasons. First, for the data not acquired with low c conditions the n values from the fits are close to 1. There are some outliers such as for MN21 where n was determined to be 0.4. These low n values likely result from an inaccurate determination of the aptamer concentration using the calculated extinction coefficient rather than not being a true 1:1 binding ratio. Most importantly, the 1:1 binding ratio for the aptamer-cocaine complex agrees with the NMR data where only one binding site is observed and there are no chemical shift perturbations above a 1:1 molar ratio. Additionally, in a cocaine titration monitored by 2D TOCSY experiments there was no evidence for multiple binding events. For the H5–H6 correlations that move with ligand binding the resonances move in a straight line as expected for a 1:1 binding ratio. Previously in our lab, a 2:1 ligand:RNA ratio was observed for paromomycin binding to a RNA molecule containing a CC mismatch [31]. Here, the TOCSY data showed distinctly curved trajectories for the H5–H6 correlations as ligand was titrated into the RNA and multiple binding sites were populated.

We also analyzed the binding thermodynamics of the two-stranded cocaine-binding aptamer (Fig. 5). Not surprising, considering their complementarity, the two DNA strands bind each other in the absence of cocaine having a K_d of 11 ± 1 μM. How does this relate to the applications that use a two-stranded aptamer as a way of assembling DNA molecules by a cocaine-binding induced folding mechanism? Many of these applications work at a DNA concentration of 10–20 μM. Therefore a significant proportion of the DNA would exist in both a bound DNA–DNA complex and as free strands. Cocaine binding then induces the folding of the free DNA strands and may also rigidify the existing DNA–DNA assemblies. This shows the importance of varying the DNA concentration in experiments that rely on the two-stranded DNA aptamer, though other experimental factors such as salt concentration also should be considered. Finally, we note the high affinity of the 1:1 mixture of the two stranded DNA aptamer (MS3/MS4) of 6 ± 1 μM. This is similar to that of MN4 despite its sequence being most similar to MN1. This may be a result of the length of helix 2 being longer in the MS3/MS4 construct than in MN1.

In summary, the data presented here demonstrate that the cocaine-binding aptamer employs a binding mechanism where ionic interactions play an important role, but do not solely govern ligand binding. The length of all three stems in the aptamer is important in ligand binding and cannot be shortened without reducing binding affinity. In contrast, increasing the length of the three stems results in an aptamer with an increased ligand affinity. This observation is consistent with our hypothesis that tertiary structure formation concurrent with ligand binding provides an important driving force for cocaine recognition.

Acknowledgments

We thank Agnesa Shala (York University, Toronto), members of the Johnson laboratory (York University, Toronto) and members of the Wilce laboratory (Monash University, Clayton, Australia) for useful discussions. This work was supported by funding from the Natural Sciences and Engineering Research Council of Canada (NSERC) to P.E.J.

Appendix A. Supplementary Data

Supplementary data to this article can be found online at doi:10.1016/j.bpc.2010.09.009.

References

[1] J. Liu, Z. Cao, Y. Lu, Functional nucleic acid sensors, Chem. Rev. 109 (2009) 1948–1998.
[2] E.J. Cho, J.-W. Lee, A.D. Ellington, Applications of aptamers as sensors, Annu. Rev. Anal. Chem. 2 (2009) 241–264.
[3] D. Li, S. Song, C. Fan, Target-responsive structural switching for nucleic acid-based sensors, Acc. Chem. Res. 43 (2010) 631–641.
[4] G. Mayer, The chemical biology of aptamers, Angew. Chem. Int. Ed. 48 (2009) 2672–2689.
[5] M.N. Stojanovic, P. de Prada, D.W. Landry, Fluorescent sensors based on aptamer self-assembly, J. Am. Chem. Soc. 122 (2000) 11547–11548.
[6] M.N. Stojanovic, P. de Prada, D.W. Landry, Aptamer-based folding fluorescent sensor for cocaine, J. Am. Chem. Soc. 123 (2001) 4928–4931.
[7] M.N. Stojanovic, D.W. Landry, Aptamer-based colorimetric probe for cocaine, J. Am. Chem. Soc. 124 (2002) 9678–9679.
[8] B.R. Baker, R.Y. Lai, M.S. Wood, E.H. Doctor, A.J. Heeger, K.W. Plaxco, An electronic, aptamer-based small-molecule sensor for the rapid, label-free detection of cocaine in adulterated samples and biological fluids, J. Am. Chem. Soc. 128 (2006) 3138–3139.
[9] J. Liu, Y. Lu, Fast colorimetric sensing of adenosine and cocaine based on a general sensor design involving aptamers and nanoparticles, Angew. Chem. Int. Ed. 45 (2006) 90–94.
[10] M. Zayats, Y. Huang, R. Gill, C. Ma, I. Willner, Label-free and reagentless aptamer-based sensors for small molecules, J. Am. Chem. Soc. 128 (2006) 13666–13667.
[11] J. Liu, J.H. Lee, Y. Lu, Quantum dot encoding of aptamer-linked nonostructures for one-pot simultaneous detection of multiple analytes, Anal. Chem. 79 (2007) 4120–4125.
[12] T. Li, B. Li, S. Dong, Adaptive recognition of small molecules by nucleic acid aptamers through a label-free approach, Chem. Eur. J. 13 (2007) 6718–6723.
[13] J. Chen, J. Jiang, X. Gao, G. Liu, G. Shen, G. Yu, A new aptameric biosensor for cocaine based on surace-enhanced raman scattering spectroscopy, Chem. Eur. J. 14 (2008) 8374–8382.
[14] J. Zhang, L. Wang, D. Pan, S. Song, F.Y.C. Boey, H. Zhang, C. Fan, Visual cocaine detection ith gold nanoparticles and rationally engineered aptamer structures, Small 4 (2008) 1196–1200.
[15] B. Madru, F. Chapuis-Hugon, E. Peyrin, V. Pichon, Determination of cocaine in human plasma by selective solid-phase extraction using an aptamer-based sorbent, Anal. Chem. 81 (2009) 7081–7086.
[16] Y. Du, C. Chen, J. Yin, B. Li, M. Zhou, S. Dong, E. Wang, Solid-state probe based electrochemical aptasensor for cocaine: a potentially convenient, sensitive, repeatable, and integrated sensing platform for drugs, Anal. Chem. 82 (2010) 1556–1563.
[17] J.E. He, Z.H. Wu, H. Zhou, H.-Q. Wang, J.-H. Jiang, G.-L. Shen, Q. YuR, Fluorescence aptameric sensor for strand displacement amplification detection of cocaine, Anal. Chem. 82 (2010) 1135–1358.
[18] M.A.D. Neves, O. Reinstein, P.E. Johnson, Defining a stem length-dependant binding mechanism for the cocaine-binding aptamer. A combined NMR and calorimetry study, Biochemistry 49 (2010) 8478–8487.
[19] P. Cekan, E.O. Jonsson, S.T. Sigurdsson, Folding of the cocaine aptamer studied by EPR and fluorescence spectroscopies using the bifunctional spectroscopic probe Ç, Nucleic Acids Res. 37 (2009) 3990–3995.
[20] R. Freeman, Y. Li, R. Tel-Vered, E. Sharon, J. Elbaz, I. Willner, Self-assembly of supramolecular aptamer structures for optical or electrochemical sensing, Analyst 134 (2009) 653–656.
[21] R. Freeman, E. Sharon, R. Tel-Vered, I. Willner, Supramolecular cocaine-aptamer complexes activate biocatalytic cascades, J. Am. Chem. Soc. 131 (2009) 5028–5029.
[22] Z.-G. Wang, O.I. Wilner, I. Willner, Self-assembly of aptamer-circular DNA nanostructures for controlled biocatalysis, Nano Lett. 9 (2009) 4098–4102.
[23] F. Delaglio, S. Grzesiek, G.W. Vuister, G. Zhu, J. Pfeifer, A. Bax, NMRPipe: a multidimensional spectral processing system based on UNIX pipes, J. Biomol. NMR 6 (1995) 277–293.
[24] W.B. Turnbull, A.H. Daranas, On the value of c: can low affinity systems be studied by isothermal titration calorimetry? J. Am. Chem. Soc. 125 (2003) 14859–14866.
[25] J. Tellinghuisen, Isothermal titration calorimetry at very low c, Anal. Biochem. 373 (2008) 395–397.
[26] H. Lu, X. Chen, C.-G. Zhan, First-principles calculation of pK for cocaine, nicotine, neurotransmitters, and anilines in aqueous solution, J. Phys. Chem. B 111 (2007) 10599–10605.
[27] M.N. Stojanovic, E.G. Green, S. Semova, D.B. Nikic, D.W. Landry, Cross-reactive arrays based on three-way junctions, J. Am. Chem. Soc. 125 (2003) 6085–6089.
[28] E. Green, M.J. Olah, T. Abramova, L.R. Williams, D. Stefanovic, T. Worgall, M.N. Stojanovic, A rational approach to minimal high-resolution cross-reactive arrays, J. Am. Chem. Soc. 128 (2006) 15278–15282.
[29] R. Pei, A. Shen, M.J. Olah, D. Stefanovic, T. Worgall, M.N. Stojanovic, High-resolution cross-reactive array for alkaloids, Chem. Commun. (2009) 3193–3195.
[30] Y.-G. Gao, H. Robinson, R. Sanishvili, A. Joachimiak, A.H.-L. Wang, Structure and recognition of sheared tandem GA base pairs associated with human centromere DNA sequence at atomic resolution, Biochemistry 38 (1999) 16452–16460.
[31] T.J. Tavares, A.V. Beribisky, P.E. Johnson, Structure of the Cytosine–Cytosine mismatch in the thymidylate synthase mRNA binding site and analysis of its interaction with the aminoglycoside paromomycin, RNA 15 (2009) 911–922.